# Emergent Information Distance from Petz Recovery

Temperature and perturbation dependence in TFIM exact diagonalization

Lluis Eriksson
Independent Researcher
lluiseriksson@gmail.com

January 2026

**Abstract**

We define an operational notion of effective distance from approximate quantum state recovery. Given a tripartition $A$–$B$–$C$ with $B$ a collar of width $w$ separating $A$ from $C$, we compute a Petz recovery reconstruction error $E_{\mathrm{Petz}}(w) = -\log F(\rho_{ABC}, \tilde{\rho}^{\mathrm{Petz}}_{ABC}(w))$ and define an emergent distance $d_{\mathrm{eff}}(\varepsilon)$ as the minimal collar width $w$ such that the best-achieved error up to $w$ falls below a target threshold $\varepsilon$. Using exact diagonalization data for the transverse-field Ising chain at $N = 11$ and $|A| = 2$, we find that $d_{\mathrm{eff}}(10^{-3})$ grows strongly with inverse temperature $\beta$ in the unperturbed case ($h_z = 0$), from 1.00 at $\beta = 0.5$ to 3.57 at $\beta = 5.0$, while it remains near-minimal in the longitudinally perturbed case ($h_z = 0.5$), staying close to 1.0 across the same temperature range. We also introduce a discrete curvature diagnostic based on second differences of $\log E_{\mathrm{Petz}}(w)$ on a pre-floor window and report when this diagnostic is identifiable given the available window and numerical floor.

## Contents

# 1 Introduction

Motivated by the general theme that locality and entanglement structure constrain information flow, we extract a quantitative, geometry-like diagnostic directly from approximate recoverability. In finite dimensions, small conditional mutual information implies the existence of good recovery channels [1, 2]. Here we take a complementary, operational route: we treat recovery performance itself as the primitive observable, and define an "effective distance" by the minimal separation needed to reach a fixed recovery-error threshold.

We emphasize scope: we do not attempt to derive gravitational field equations. The goal is a minimal, falsifiable construction of an emergent geometric diagnostic from recovery error in a concrete lattice setting.

# 2 Setup and definitions

We consider a 1D chain and a tripartition $A$–$B$–$C$, where $B$ is a collar of width $w$ separating $A$ from $C$. For each $w$ we form a Petz-based reconstructed state $\widetilde{\rho}^{\mathrm{Petz}}_{ABC}(w)$ by applying the Petz map to the input marginal $\rho_{AB}$, using $\rho_{BC}$ (and hence $\rho_B$) as reference marginals extracted from the same target state $\rho_{ABC}$. We define the Petz error

$$E_{\mathrm{Petz}}(w) := -\log F\big(\rho_{ABC}, \widetilde{\rho}^{\mathrm{Petz}}_{ABC}(w)\big)\,,$$

where $F(\rho,\sigma)$ is the (squared) Uhlmann fidelity

$$F(\rho,\sigma) := \left(\mathrm{Tr}\sqrt{\sqrt{\rho}\,\sigma\,\sqrt{\rho}}\right)^2.$$

**Petz recovery map (operational definition).** We use the Petz map for the channel $\mathrm{Tr}_C$ [3],

$$\widetilde{\rho}^{\mathrm{Petz}}_{ABC} = (\mathrm{id}_A \otimes \mathcal{R}^{\mathrm{Petz}}_{B\to BC})(\rho_{AB}), \qquad \mathcal{R}^{\mathrm{Petz}}_{B\to BC}(X_B) = \rho_{BC}^{1/2}\,\rho_B^{-1/2}\,X_B\,\rho_B^{-1/2}\,\rho_{BC}^{1/2},$$

where $\rho_B = \mathrm{Tr}_A(\rho_{AB})$. Matrix inverse powers are computed via spectral decomposition with an eigenvalue floor $\lambda \mapsto \max(\lambda, \lambda_{\min})$ applied only when forming $\rho_B^{-1/2}$ (we use $\lambda_{\min} = 10^{-12}$) to stabilize the inverse when $\rho_B$ has small eigenvalues. The factor $\rho_{BC}^{1/2}$ does not require inversion and is computed as a positive square root.

Numerically, after constructing $\widetilde{\rho}^{\mathrm{Petz}}_{ABC}$ we hermitize it via $X \mapsto (X + X^\dagger)/2$. To ensure that the recovered operator is a valid density matrix, we then project to the positive semidefinite cone by spectral decomposition, $\widetilde{\rho} = \sum_j \lambda_j |\psi_j\rangle\langle\psi_j| \mapsto \sum_j \max(\lambda_j, 0)\,|\psi_j\rangle\langle\psi_j|$, and finally renormalize to unit trace. We report $E_{\mathrm{Petz}}(w)$ using this PSD-projected, renormalized output. In a direct check at $N = 11$ with $w \le 5$ for $h_z \in \{0, 0.5\}$ and $\beta \in \{1, 5\}$, this post-processing changes $E_{\mathrm{Petz}}(w)$ by at most $\sim 3 \times 10^{-8}$ in absolute value. This avoids numerical pathologies when evaluating $F(\rho, \widetilde{\rho})$.

To stabilize finite-size/non-monotone artifacts, define

$$E_{\mathrm{best}}(w) := \min_{w' \le w} E_{\mathrm{Petz}}(w').$$

For a target threshold $\varepsilon > 0$, define the effective distance

$$d_{\mathrm{eff}}(\varepsilon) := \min\{w :\ E_{\mathrm{best}}(w) \le \varepsilon\}.$$

When needed, we use log-linear interpolation between adjacent $w$ values to obtain a real-valued estimate.

**Pre-floor window and curvature diagnostic.** Let $y_{\min} := 10^{-12}$ denote the numerical floor used for censoring/visualization of $E_{\mathrm{Petz}}(w)$ in log-scale plots. We define the *pre-floor window* by $E_{\mathrm{Petz}}(w) \geq 10\, y_{\min}$. This $y_{\min}$ is distinct from the spectral regularization floor $\lambda_{\min}$ used when computing $\rho_B^{-1/2}$ in the Petz map. On this window we define the discrete curvature

$$\kappa(w) := \big(\log E_{\mathrm{Petz}}(w{+}1) - \log E_{\mathrm{Petz}}(w)\big) - \big(\log E_{\mathrm{Petz}}(w) - \log E_{\mathrm{Petz}}(w{-}1)\big),$$

and summarize it by $\bar{\kappa} = \langle|\kappa(w)|\rangle$ when at least three consecutive collar widths lie in the pre-floor window.

# 3 Data and methodology

## 3.1 Model and numerics

We analyze exact diagonalization data for the transverse-field Ising chain with a longitudinal perturbation [4]. We use open boundary conditions and fix $J = 1$ as the energy scale. The Hamiltonian is

$$H = -J \sum_{i=1}^{N-1} Z_i Z_{i+1} - h_x \sum_{i=1}^{N} X_i - h_z \sum_{i=1}^{N} Z_i,$$

with $h_x = 1.05$ throughout and $h_z \in \{0, 0.5\}$ defining the two regimes studied.

For each inverse temperature $\beta$, we consider the Gibbs state

$$\rho = \frac{e^{-\beta H}}{\mathrm{Tr}(e^{-\beta H})}.$$

We obtain $\rho$ by exact diagonalization of $H$ and compute reduced density matrices by partial traces.

**Tripartition geometry.** We choose contiguous subsystems along the chain with $|A| = 2$ at the left edge and a collar $B$ of width $w$ adjacent to $A$. Concretely, $A = \{1, 2\}$, $B = \{3, \ldots, 2 + w\}$ and $C = \{3 + w, \ldots, N\}$. The accessible collar window is $w \in \{1, 2, 3, 4, 5\}$ at system size $N = 11$.

## 3.2 Pre-floor fits and identifiability

To quantify decay of the recovery error before saturation, we fit $\log E_{\mathrm{Petz}}(w) \approx a - \mu_{\mathrm{prefloor}}\, w$ on the pre-floor window (when at least two points are available). We report identifiability of curvature diagnostics via $(n_{\mathrm{prefloor}}, n_\kappa)$.

**Reproducibility.** The Overleaf bundle may include a flattened CSV (`flattened_data.csv`), a summary CSV (`summary_table_with_kappa.csv`), and (for the appendix) a size-check table fragment (`table_sizecheck.tex`). The PSD-projection sensitivity check (yielding the $\sim 3 \times 10^{-8}$ bound) was performed by rerunning the computation with a patched driver ($\texttt{run}_e d_p sdproj.py) that applies PSD projection and trac

# 4 Results

## 4.1 Recovery error profiles

Figure 1 shows $E_{\mathrm{Petz}}(w)$ as a function of collar width for representative inverse temperatures and for two regimes, $h_z = 0$ and $h_z = 0.5$.

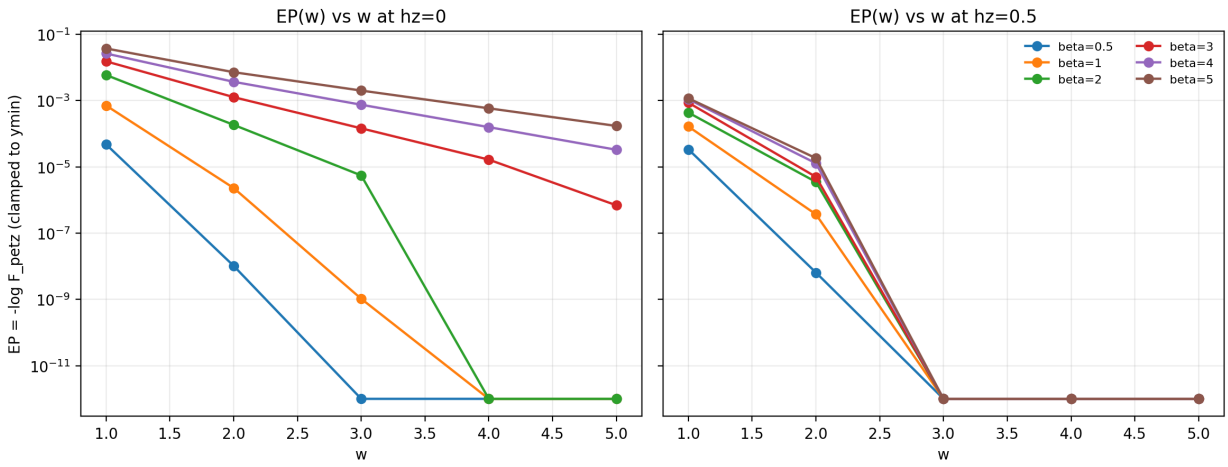


Figure 1: $E_{\mathrm{Petz}}(w)$ versus collar width $w$, shown on a log scale. For visualization we clamp values below $y_{\min} = 10^{-12}$. Left: $h_z = 0$. Right: $h_z = 0.5$.

### 4.2 Effective distance scaling with temperature

At threshold $\varepsilon = 10^{-3}$ we observe a strong growth of $d_{\mathrm{eff}}(\varepsilon)$ with $\beta$ for $h_z = 0$, while $d_{\mathrm{eff}}(\varepsilon)$ remains near-minimal for $h_z = 0.5$:

$$d_{\mathrm{eff}}(10^{-3}) = \begin{cases} 1.00,\ 1.00,\ 1.51,\ 2.11,\ 2.82,\ 3.57 & (h_z = 0,\ \ \beta = 0.5, 1, 2, 3, 4, 5), \\ 1.00,\ 1.00,\ 1.00,\ 1.00,\ 1.02,\ 1.04 & (h_z = 0.5,\ \ \beta = 0.5, 1, 2, 3, 4, 5). \end{cases}$$

See Figure 2.

### 4.3 Sensitivity to the threshold $\varepsilon$

To verify that the qualitative separation between $h_z = 0$ and $h_z = 0.5$ is not an artifact of a single choice of threshold, we also compute $d_{\mathrm{eff}}(\varepsilon)$ for $\varepsilon \in \{10^{-2}, 10^{-3}, 10^{-4}\}$. Within the available collar window $w \leq 5$, the ordering between the two regimes remains stable across these thresholds (see Figure 3).

In particular, for the tested $\varepsilon$ we find $d_{\mathrm{eff}\,h_z=0}(\varepsilon) \geq d_{\mathrm{eff}\,h_z=0.5}(\varepsilon)$ for all sampled $\beta$, with a clear separation at larger $\beta$ within the available collar window.

### 4.4 Decay-rate proxy and curvature identifiability

A log-linear pre-floor fit yields an effective decay-rate proxy $\mu_{\mathrm{prefloor}}$ which decreases strongly with $\beta$ at $h_z = 0$ (from $\mu_{\mathrm{prefloor}} \approx 8.44$ at $\beta = 0.5$ to $\mu_{\mathrm{prefloor}} \approx 1.33$ at $\beta = 5$), while remaining comparatively large at $h_z = 0.5$ (roughly $\mu_{\mathrm{prefloor}} \in [4.16, 8.56]$ across $\beta$).

We also report the curvature summary $\bar{\kappa}$ when identifiable. For $h_z = 0.5$, the pre-floor window contains only $n_{\mathrm{prefloor}} = 2$ points, so $n_\kappa = 0$ and $\bar{\kappa}$ is not defined in the pre-floor sense. For $h_z = 0$ and $\beta \geq 1$, curvature is identifiable with $(n_{\mathrm{prefloor}}, n_\kappa) \in \{(3, 1), (5, 3)\}$ and $\bar{\kappa}$ is nontrivial (e.g. $\bar{\kappa} \approx 1.97$ at $\beta = 1$ and $\bar{\kappa} \approx 0.44$ at $\beta = 3$).

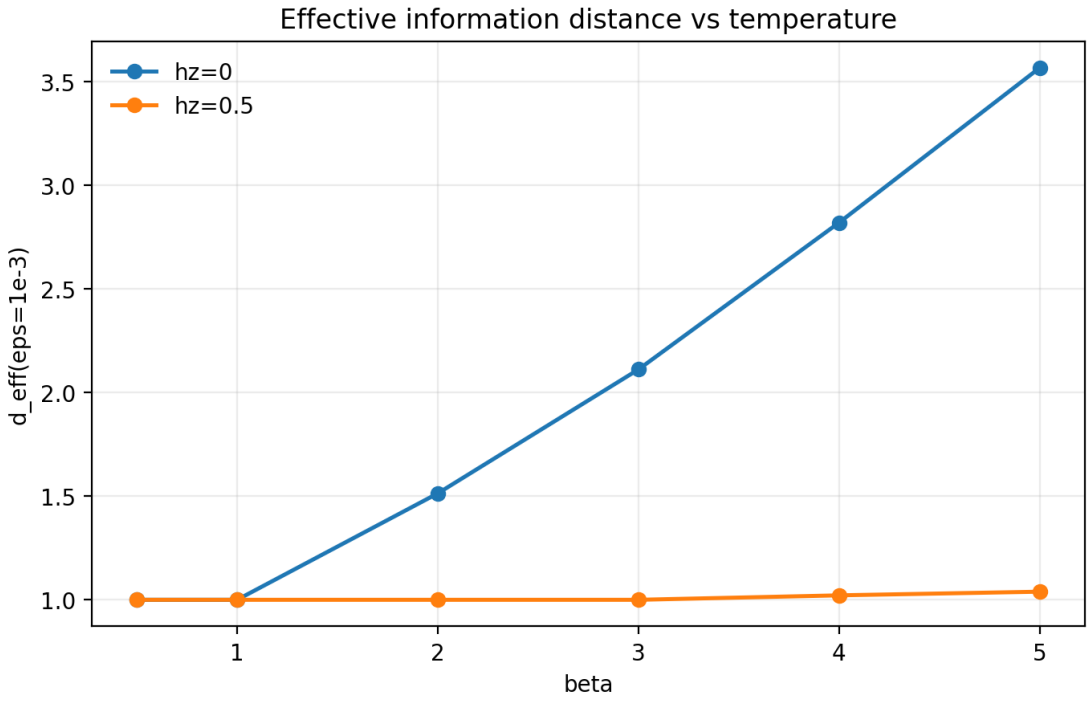


Figure 2: Effective distance $d_{\text{eff}}(10^{-3})$ versus inverse temperature $\beta$ for $h_z = 0$ and $h_z = 0.5$.

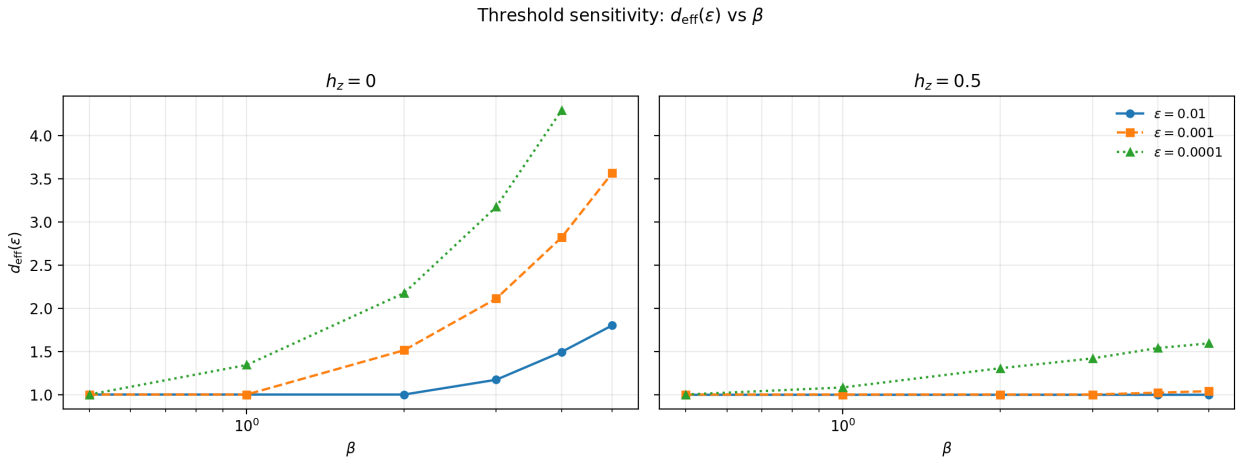


Figure 3: Threshold sensitivity of the recovery distance: $d_{\text{eff}}(\varepsilon)$ versus $\beta$ for multiple values of $\varepsilon$ in both regimes $h_z = 0$ and $h_z = 0.5$.

| $h_z$ | $\beta$ | $d_{\mathrm{eff}}(10^{-3})$ | $\mu_{\mathrm{prefloor}}$ | $n_{\mathrm{prefloor}}$ | $n_\kappa$ | $\bar{\kappa}$ | $\#(E_{\mathrm{Petz}} = 0)$ | $\#(E_{\mathrm{Petz}} < y_{\min})$ |
|---|---|---|---|---|---|---|---|---|
| 0.0 | 0.5 | 1.000000 | 8.440418 | 2 | 0 | – | 1 | 3 |
| 0.0 | 1.0 | 1.000000 | 6.716149 | 3 | 1 | 1.965259 | 2 | 2 |
| 0.0 | 2.0 | 1.513419 | 3.488846 | 3 | 1 | 0.050901 | 2 | 2 |
| 0.0 | 3.0 | 2.111198 | 2.434588 | 5 | 3 | 0.441875 | 0 | 0 |
| 0.0 | 4.0 | 2.819732 | 1.652564 | 5 | 3 | 0.142798 | 0 | 0 |
| 0.0 | 5.0 | 3.566592 | 1.327455 | 5 | 3 | 0.140969 | 0 | 0 |
| 0.5 | 0.5 | 1.000000 | 8.562682 | 2 | 0 | – | 2 | 3 |
| 0.5 | 1.0 | 1.000000 | 6.100816 | 2 | 0 | – | 3 | 3 |
| 0.5 | 2.0 | 1.000000 | 4.817792 | 2 | 0 | – | 3 | 3 |
| 0.5 | 3.0 | 1.000000 | 5.155266 | 2 | 0 | – | 3 | 3 |
| 0.5 | 4.0 | 1.021467 | 4.450958 | 2 | 0 | – | 3 | 3 |
| 0.5 | 5.0 | 1.039167 | 4.162260 | 2 | 0 | – | 3 | 3 |

Table 1: Summary of effective distance, pre-floor decay-rate proxy, and curvature identifiability. The pre-floor window is defined by $E_{\mathrm{Petz}}(w) \geq 10\, y_{\min}$ with $y_{\min} = 10^{-12}$.

# 5 Limitations and outlook

**Systematic uncertainties.** Reported values of $d_{\mathrm{eff}}(\varepsilon)$ are affected by finite collar resolution ($w \in \{1, \ldots, 5\}$) and by the use of log-linear interpolation between adjacent collar widths when $E_{\mathrm{best}}(w)$ crosses the threshold. We therefore interpret variations below $\Delta w \sim 0.1$ as below resolution and emphasize robust qualitative trends.

**PSD projection as numerical post-processing.** To guarantee a valid density matrix before evaluating $F(\rho, \widetilde{\rho})$, we apply a PSD projection and trace renormalization to the Petz output. In a direct check at $N = 11$ with $w \leq 5$ for $h_z \in \{0, 0.5\}$ and $\beta \in \{1, 5\}$, this post-processing changes $E_{\mathrm{Petz}}(w)$ by at most $\sim 3{\times}10^{-8}$ in absolute value and does not affect any qualitative trends reported here.

The present study is limited by the finite-size collar window $w \leq 5$ at $N = 11$ and by numerical floors. Nevertheless, the recovery-based distance $d_{\mathrm{eff}}(\varepsilon)$ provides a compact operational diagnostic whose qualitative dependence on $\beta$ and $h_z$ persists across multiple thresholds $\varepsilon$. A minimal finite-size robustness check at $N = 12$ is provided in Section A.

Future work includes extending the collar window using tensor-network methods, comparing Petz-based recovery to existence-certified bounds, and testing whether recoverability-based distances satisfy additional metric-like properties under composition and coarse-graining.

# A Finite-size robustness check ($N = 11$ vs $N = 12$)

We perform a minimal finite-size robustness check by comparing $N = 11$ and $N = 12$ at $\beta \in \{1, 5\}$ for $h_z \in \{0, 0.5\}$, keeping the same geometry ($|A| = 2$) and collar window $w \in \{1, 2, 3, 4, 5\}$. We report $d_{\mathrm{eff}}(10^{-3})$ together with pre-floor identifiability counters $(n_{\mathrm{prefloor}}, n_\kappa)$, where $n_{\mathrm{prefloor}}$ counts the number of collar widths satisfying $E_{\mathrm{Petz}}(w) \geq 10\, y_{\min}$ and $n_\kappa$ counts how many discrete curvature points $\kappa(w)$ can be formed from three consecutive pre-floor widths.

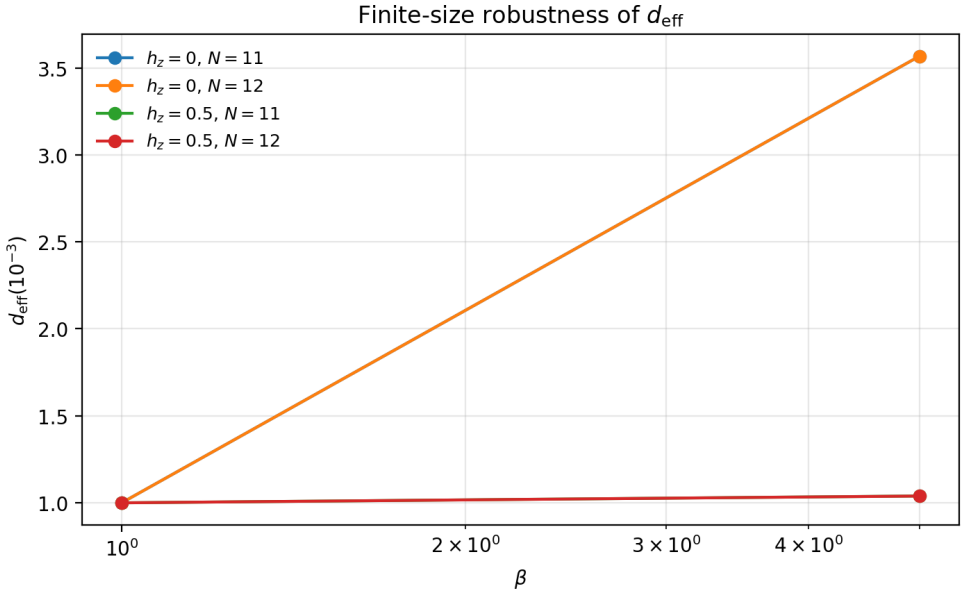


Figure 4: Finite-size robustness of $d_{\mathrm{eff}}(10^{-3})$ comparing $N = 11$ and $N = 12$ at $\beta \in \{1, 5\}$ for $h_z \in \{0, 0.5\}$. The qualitative separation between the unperturbed case ($h_z = 0$) and the longitudinally perturbed case ($h_z = 0.5$) is preserved.

| $h_z$ | $\beta$ | $N$ | $d_{\mathrm{eff}}(10^{-3})$ | $\mu_{\mathrm{prefloor}}$ | $n_{\mathrm{prefloor}}$ | $n_\kappa$ | $\bar{\kappa}$ |
|---|---|---|---|---|---|---|---|
| 0.0 | 1.0 | 11 | 1.000 | 6.716 | 3 | 1 | 1.965 |
| 0.0 | 1.0 | 12 | 1.000 | 5.737 | 2 | 0 | — |
| 0.0 | 5.0 | 11 | 3.567 | 1.327 | 5 | 3 | 0.141 |
| 0.0 | 5.0 | 12 | 3.567 | 1.328 | 5 | 3 | 0.140 |
| 0.5 | 1.0 | 11 | 1.000 | 6.101 | 2 | 0 | — |
| 0.5 | 1.0 | 12 | 1.000 | 6.192 | 2 | 0 | — |
| 0.5 | 5.0 | 11 | 1.039 | 4.162 | 2 | 0 | — |
| 0.5 | 5.0 | 12 | 1.039 | 4.179 | 2 | 0 | — |

Table 2: Finite-size robustness summary. When $n_\kappa = 0$, $\bar{\kappa}$ is not reported (not identifiable on the pre-floor window).

## References


[1] Omar Fawzi and Renato Renner. Quantum conditional mutual information and approximate markov chains. *Communications in Mathematical Physics*, 340:575-611, 2015.

[2] Marius Junge, Renato Renner, David Sutter, Mark M. Wilde, and Andreas Winter. Universal recovery maps and approximate sufficiency of quantum relative entropy. *Annales Henri Poincare*, 19:2955-2978, 2018.

[3] Dénes Petz. Sufficient subalgebras and the relative entropy of states of a von neumann algebra. *Communications in Mathematical Physics*, 105:123-131, 1986.

[4] Subir Sachdev. *Quantum Phase Transitions*. Cambridge University Press, 2 edition, 2011.